Involvement of cathepsin B in the plant disease resistance hypersensitive response

The Plant Journal (2007) **52**, 1–13 doi: 10.1111/j.1365-313X.2007.03226.x

Involvement of cathepsin B in the plant disease resistance hypersensitive response

Eleanor M. Gilroy[1], Ingo Hein[1], Renier van der Hoorn[2], Petra C. Boevink[1], Eduard Venter[1,†], Hazel McLellan[1,3], Florian Kaffarnik[4], Katarina Hrubikova[1], Jane Shaw[1], Maria Holeva[1], Eduardo C. López[5], Orlando Borras-Hidalgo[5], Leighton Pritchard[1], Gary J. Loake[3], Christophe Lacomme[1,3] and Paul R. J. Birch[1,*]

[1]*Plant Pathology Programme, Scottish Crop Research Institute, Invergowrie, Dundee DD2 5DA, UK,*

[2]*Max Planck Institute for Plant Breeding Research, Carl-von-Linné-Weg 10, 50829 Cologne, Germany,*

[3]*Institute of Molecular Plant Sciences, School of Biological Sciences, Edinburgh University, King's Buildings, Mayfield Road, Edinburgh EH9 3JR, UK,*

[4]*Sainsbury Laboratory, John Innes Centre, Norwich NR5 7UH, UK, and*

[5]*Center for Genetic Engineering and Biotechnology (C.I.G.B.), Ave. 31 e/ 158 y 190, Playa, Havana 10600, Cuba*

Received 30 March 2007; revised 15 May 2007; accepted 23 May 2007.

[*]For correspondence (fax +44 1382 568578; e-mail: pbirch@scri.sari.ac.uk).

[†]Present address: Department of Botany and Plant Biotechnology, University of Johannesburg, Johannesburg, South Africa.

Summary

A diverse range of plant proteases are implicated in pathogen perception and in subsequent signalling and execution of disease resistance. We demonstrate, using protease inhibitors and virus-induced gene silencing (VIGS), that the plant papain cysteine protease cathepsin B is required for the disease resistance hypersensitive response (HR). VIGS of cathepsin B prevented programmed cell death (PCD) and compromised disease resistance induced by two distinct non-host bacterial pathogens. It also suppressed the HR triggered by transient co-expression of potato *R3a* and *Phytophthora infestans Avr3a* genes. However, VIGS of cathepsin B did not compromise HR following recognition of *Cladosporium fulvum* AVR4 by tomato Cf-4, indicating that plant PCD can be independent of cathepsin B. The non-host HR to *Erwinia amylovora* was accompanied by a transient increase in cathepsin B transcript level and enzymatic activity and induction of the HR marker gene *Hsr203*. VIGS of cathepsin B significantly reduced the induction of *Hsr203* following *E. amylovora* challenge, further demonstrating a role for this protease in PCD. Whereas cathepsin B is often relocalized from the lysosome to the cytosol during animal PCD, plant cathepsin B is secreted into the apoplast, and is activated upon secretion in the absence of pathogen challenge.

Keywords: papain, apoptosis, protease, non-host, gene-for-gene.

Introduction

Plants have pre-formed barriers and inducible innate immune systems that prevent infection by most pathogenic micro-organisms (Nürnberger and Lipka, 2005; Hye-Sook and Collmer, 2005). A component of disease resistance that is often induced is the hypersensitive response (HR), a form of localized programmed cell death (PCD). The HR may be triggered in non-host resistance, i.e. in plants that are challenged by micro-organisms that are pathogens of other plant species (Alfano and Collmer, 2004). In addition, pathogen recognition through interactions of plant resistance (*R*) gene products and corresponding pathogen avirulence (*Avr*) gene products may induce HR in what is known as a gene-for-gene interaction (Greenberg and Yao, 2004). Absence of corresponding alleles of the *R* gene in the host or the *Avr* gene in the pathogen leads to a compatible (susceptible) interaction.

Although little is understood about the regulatory and mechanistic processes underlying inducible disease resistance, extracellular and intracellular proteases play diverse, fundamental roles during pathogen recognition and induction of defences (Van der Hoorn and Jones, 2004). Indeed, some proteases may be suppressed by pathogen protease inhibitors during infection. Examples include an apoplastic papain-like protease from *Lycopersicon esculentum*, RCR3,

which is a putative virulence target of the protease inhibitor, AVR2, from the fungal pathogen *Cladosporum fulvum* (Rooney *et al.*, 2005). This molecular interaction is perceived by tomato R protein, Cf-2, leading to a HR. A subtilisin-like protease and pathogenesis related (PR) protein, P69B, is involved in proteolytic defence responses in the plant extracellular matrix (Tornero *et al.*, 1996, 1997). P69B is targeted directly by a Kazal-like extracellular serine protease inhibitor from the *Solanum tuberosum* late blight pathogen *Phytophthora infestans* (Tian *et al.*, 2004). Moreover, recently it has been demonstrated that a cystatin from *P. infestans*, EPIC2, interacts with and inhibits a novel papain-like cysteine protease, PIP1, which is a PR protein closely related to RCR3 (Tian *et al.*, 2007).

In animals, a form of PCD called apoptosis involves cysteine proteases called caspases that cleave a limited set of cellular protein substrates (Thornberry and Lazebnik, 1998). Caspase knockouts or caspase inhibitors counteract apoptosis in animals. Since the plant HR and apoptosis share many physiological and morphological features, it is reasonable to predict that protease components of PCD may be conserved between the kingdoms. Thus, caspase inhibitors and substrates from animal research were used to demonstrate that caspase-like activities are induced during HR and that caspase inhibitors block the HR (Del Pozo and Lam, 1998; Chichkova *et al.*, 2004; Woltering, 2004). However, plants lack homologues of caspase genes, and recent reports indicate that plant proteases with caspase-like activities belong to different families. Vacuolar processing enzyme (VPE) exhibiting caspase-1-like activity during Tobacco mosaic virus-mediated HR in tobacco (Hatsugai *et al.*, 2004) is a member of the C13 family, structurally related to caspases (C14), and subtilisin-like serine proteases (family S8) exhibiting caspase specificity (saspases) are activated during PCD induced by a plant pathogen-derived toxin, victorin (Coffeen and Wolpert, 2004). Nevertheless, protease inhibitors such as E64, AEBSF and TLCK, that do not inhibit plant caspase activities, can still block plant cell death, suggesting that additional proteases, such as papain-like proteases, are effectors or regulators of plant PCD (D'Silva *et al.*, 1998; Coffeen and Wolpert, 2004; Woltering, 2004).

Additional proteases shown to play a role in plant disease resistance include the extracellular aspartate protease, CDR1 (Xia *et al.*, 2004). Antisense *CDR1* plants were compromised in resistance to avirulent *Pseudomonas syringae*, whereas over-expression led to increased resistance to virulent *P. syringae.* CDR1 is structurally related to cathepsin D (Xia *et al.*, 2004). We have demonstrated that a potato cathepsin B-encoding gene, *StCathB*, is rapidly upregulated specifically by resistance (*R*) gene-mediated HRs elicited by *P. infestans* (Avrova *et al.*, 2004). Cathepsin B is structurally unrelated to cathepsin D, being a member of the papain family of cysteine proteases. Cathepsin B has been implicated in many diverse roles in animals, including PCD (Zeiss, 2003). In animals, cathepsin B can activate caspases (Kingham and Pocock, 2001; Vancompernolle *et al.*, 1998), and cathepsin B knockout mice fail to exhibit apoptosis (Guicciardi *et al.*, 2001; Zeiss, 2003). Nevertheless, cathepsin B can cause PCD independently of caspases (Foghsgaard *et al.*, 2001). It was thus reasonable to regard cathepsin B as a candidate cysteine protease involved in plant disease resistance.

We showed, using cathepsin B inhibitors and virus-induced gene silencing (VIGS), that cathepsin B plays a role in both host and non-host plant disease resistance. We determined that cathepsin B transcription and enzymatic activity are induced during the HR, and showed that suppression of the HR by silencing of cathepsin B significantly reduces the induction of the HR marker gene *HSR203.* Finally, we demonstrated, by using activity profiling (Van der Hoorn *et al.*, 2004) and C-terminal monomeric red fluorescent protein (mRFP) fusion, that cathepsin B is activated upon secretion into the plant apoplast, in the absence of pathogen challenge.

Results

Cathepsin B inhibitors suppress non-host disease resistance

Nicotiana species are non-hosts for the apple pathogen *Erwinia amylovora* (*Eam*), which elicits a rapid HR. To investigate the potential involvement of cathepsin B in *Eam*-mediated non-host disease resistance, we used inhibitors described in the animal literature as cathepsin B specific, z-FA-fmk, Ac-LVK-cho, CA-074-Me and the broad cathepsin B, S, L and papain inhibitor Z-FGNHO-Bz. Each inhibitor was infiltrated with 10^6 colony forming units (cfu) ml^{-1} of *Eam* into *Nicotiana benthamiana* leaves. In the absence of inhibitor, *Eam* elicited a visible HR by 24–48 h post-infiltration (hpi). In contrast, the HR was abolished or considerably reduced and delayed after infiltration of *Eam* with cathepsin B or general papain inhibitors (Figure 1a).

Two of the cathepsin B inhibitors (Ac-LVK-cho and Ca-074-Me) were selected to investigate whether they compromised disease resistance to *Eam* by measuring accumulation of viable *Eam* cells at 4 days post-infiltration (dpi). Each inhibitor resulted in approximately 10-fold increased recovery of viable bacterial cells (Figure 1b). When *Eam* was grown in King's broth in the presence or absence of cathepsin B inhibitors no significant differences in growth curves were observed (results not shown), excluding the possibility that the presence of the inhibitors had an effect on bacterial growth *in vitro*. Thus, cathepsin B inhibitors considerably reduced non-host disease resistance in *N. benthamiana* to *Eam* and resulted in a visible reduction in HR-like cell death.

To investigate the specificity of the cathepsin B inhibitors, we performed protease activity profiling. We used DCG-04, a biotinylated derivative of E-64, which inhibits papain-like proteases in an activity-dependent manner (Van der Hoorn

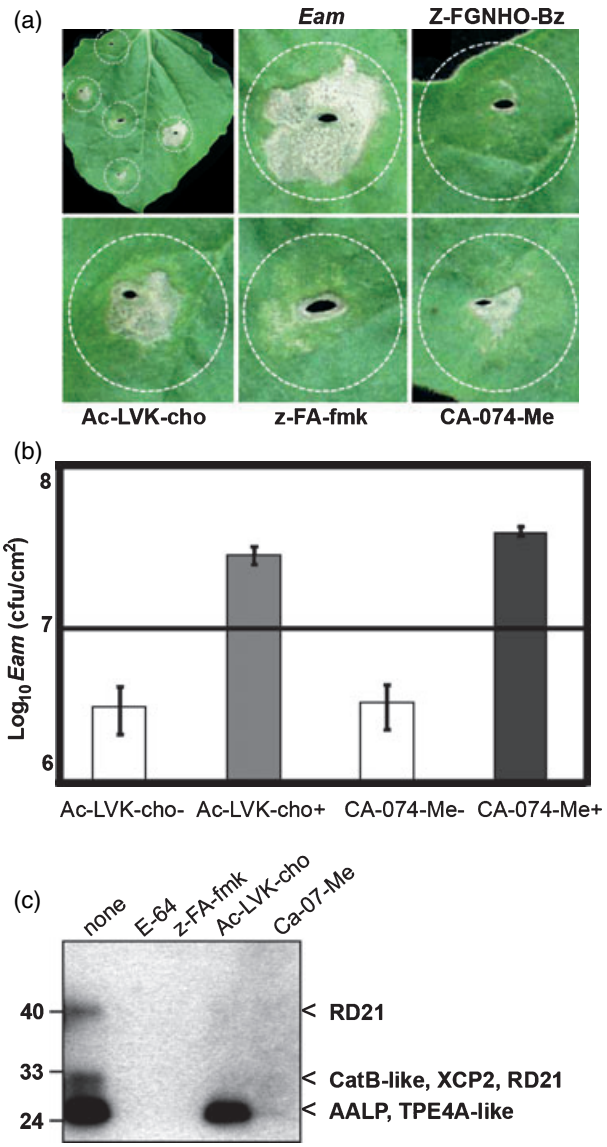

Figure 1. Cathepsin B inhibitors suppress disease resistance to *Erwinia amylovora* (*Eam*).
(a) The hypersensitive response induced by infiltration of 10^6 colony-forming units (cfu) ml^{-1} *Eam* was compromised by infiltration of *Eam* with 1 mM of the inhibitors Z-FGNHO-Bz, z-FA-fmk, Ac-LVK-cho and CA-074-Me. Zones of infiltration are indicated by dotted circles.
(b) Increases in viable *Eam* colonies recovered from leaves 4 days post-infiltration of *Eam* with 1 mM z-FA-fmk, Ac-LVK-cho or CA-074-Me, were observed relative to recovery from leaves infiltrated only with *Eam*. Results are each the mean ± SEM of three independent experiments each involving six replicate plants.
(c) Specificity of cathepsin B inhibitors was investigated by proteases activity profiling of Arabidopsis leaf extract with the biotinylated DCG-04 in the presence or absence of 0.4 mM inhibitors E-64, z-FA-fmk, Ac-LVK-cho and Ca-074-Me.

et al., 2004). Incubation of this probe with Arabidopsis leaf extracts results in three major signals on a blot probed with streptavidin-horseradish peroxidase (HRP) (Figure 1c, first lane). These signals are known to represent six different papain-like cysteine proteases, including cathepsin B in the 30 kDa region (indicated on the right in Figure 1c) (Van der Hoorn *et al.*, 2004). We used this assay to investigate the specificity of cathepsin B inhibitors. The presence of E-64, z-FA-fmk and Ca-074-Me prohibited labelling of all six proteases, whereas inhibitor Ac-LVK-cho only prevented labelling of RD21, cathepsin B, and XCP2 (Figure 1c, lanes 2–5). This indicates that whilst inhibitors z-FA-fmk, Ac-LVK-cho and Ca-074-Me block cathepsin B activity, they also inhibit other papain-like cysteine proteases. Since the role of cathepsin B in non-host resistance was inconclusive from these inhibitor studies, we embarked on VIGS to interfere specifically with cathepsin B function.

Virus induced gene silencing of cathepsin B

NbCathB, encoding cathepsin B, was cloned from *N. benthamiana*. The putative protein encoded by *NbCathB* was aligned with cathepsin B proteins from *Nicotiana rustica*, *Solanum tuberosum*, *Arabidopsis thaliana* and *Homo sapiens* and revealed that the expected peptidase C1 and propeptidase C1 cleavage domains were conserved (Supplementary Figure S1a). Publicly available expressed sequence tag (EST) databases contained, respectively, four and two independent contigs annotated as full-length cathepsin B in the closely related solanaceous species, potato (TC137447, TC145097, TC152070 and TC142279) and tomato (TC175119, TC182010). Indeed, there are three independent genes annotated as cathepsin B in *A. thaliana* [NM_100110 (*At1 g02300*); NM_100111 (*At1 g02305*); NM_116392 (*At4 g01610*)]. In each case, these genes are highly related (Supplementary Figure S1b), implying the involvement of gene families in the production of plant cathepsin B. The cathepsin B EST sequences from potato and tomato are highly similar (80–98% nucleotide (nt) identity), precluding the design of VIGS constructs that discriminate the sequences. Constructs were thus designed that were likely to silence the entire cathepsin B gene family in *N. benthamiana* whilst avoiding 'off-target' silencing of additional genes. Using the siRNA scan website (http://bioinfo2.noble.org/RNAiScan.htm; Xu *et al.*, 2006), two independent portions, of 364 and 247 bp (Supplementary Figure S1a), of *NbCathB* were screened against EST datasets from *N. benthamiana,* and from tomato, potato and tobacco to seek 22 nt stretches of homology with other genes and thus the potential for 'off-target' silencing. For both selected portions, hits were made only to sequences annotated as cathepsin B in each dataset [EST contig TC9934 (DQ492297) in *N. benthamiana*; NP917849 (AF359422) in tobacco; and all the EST contigs in potato and tomato]. It was thus unlikely that the sequences would silence genes other than cathepsin B. To further assess the potential for off-target silencing from a fully sequenced plant genome, equivalent

protein-coding portions (Supplementary Figure S1a) of each of the three *A. thaliana* genes annotated as cathepsin B were screened against all *A. thaliana* coding sequences. In each case, the query sequence showed matches only to itself and the other two cathepsin B family members, further confirming the unlikelihood of silencing genes other than cathepsin B, and indicating that the portions would silence all cathepsin B homologues in *A. thaliana*. The 364-bp and 247-bp portions of *NbCathB* were cloned in antisense orientation into a Tobacco rattle virus (TRV) vector for VIGS (construct TRV::*NbCathB-1* and TRV:*NbCathB-2* respectively) with the intention of, in each case, silencing all *NbCathB* homologues within *N. benthamiana*.

To assess the effect of silencing *NbCathB* genes on the HR, comparisons were made with plants inoculated with TRV either harbouring, as a negative control, *gfp* (TRV::*gfp*) or, as a positive control, a portion cloned in antisense of the *N. benthamiana sgt1b* cDNA (TRV::*Nbsgt1*), encoding a ubiquitin ligase-associated protein shown previously to be involved in both host and non-host plant disease resistance (Peart *et al.*, 2002).

Nicotiana benthamiana plants inoculated with TRV::*NbCathB-1*, TRV::*NbCathB-2* or TRV::*gfp* showed no discernible altered phenotype. In contrast, as observed previously (Peart *et al.*, 2002), *Nbsgt1*-silenced plants were shorter and more branched. Real-time RT-PCR revealed an approximately 90% reduction in transcript level of *NbCathB* in plants 21 days after inoculation (dai) with TRV::*NbCathB-1* or TRV::*NbCathB-2,* compared with levels 21 dai with TRV::*gfp* (Supplementary Figure S2a). Western blot analysis confirmed that *Nbsgt1* was silenced, as SGT1 protein was significantly less abundant in leaves from plants 21 dai with TRV::*sgt1b* than in plants 21 dai with TRV::*gfp* (Supplementary Figure S2b).

VIGS of cathepsin B confirms its role in non-host disease resistance

Nicotiana benthamiana plants inoculated with the TRV constructs were infiltrated with either 10^6 or 10^7 cfu ml^{-1} of *Eam*. At 24 to 48 hpi a clear HR-like cell death was visible on plants harbouring TRV::*gfp* (Figure 2a), as witnessed for non-TRV-inoculated plants (Figure 1a). However, in plants inoculated with TRV::*NbCathB-1* the *Eam*-mediated HR was abolished at the lower concentration (10^6 cfu ml^{-1}), and weak or delayed until 72 hpi at the higher concentration (10^7 cfu ml^{-1}) of bacteria (Figure 2a). Suppression of *Eam*-mediated HR by silencing *NbCathB* was similar to that observed after silencing *Nbsgt1* (results not shown).

Accumulation of viable *Eam* was measured 4 dpi. In leaves inoculated with TRV::*NbCathB-1* or TRV::*Nbsgt1*, approximately eight-fold more viable *Eam* cells were recovered in each case than in plants inoculated with TRV::*gfp* (Figure 2b). This demonstrates that silencing of *NbCathB* compromises non-host disease resistance to a level similar to that caused by silencing *Nbsgt1* (Figure 2b). Silencing *NbCathB* with the TRV::*NbCathB-2* construct resulted in a similar suppression of HR and increase in viable *Eam* cells (Supplementary Figure S3).Given the similar results with both *NbCathB* silencing constructs, further experiments were conducted using only the TRV::*NbCathB-1* construct.

Pseudomonas syringae pv. tomato (*Pst*) DC3000, when infiltrated into *N. benthamiana* at high concentrations (10^6 cfu ml^{-1}) elicits a non-host HR (Hye-Sook and Collmer, 2005). Whilst this HR was clearly visible in plants inoculated with TRV::*gfp* within 48 hpi (Figure 2c), it was suppressed in plants inoculated with either TRV::*NbCathB-1* (Figure 2c) or TRV::*Nbsgt1* (results not shown). Again, this resulted in significant (approximately five-fold in each case) increase in viable cells from TRV::*NbCathB-1* or TRV::*Nbsgt1* plants, demonstrating that disease resistance was compromised by silencing these genes (Figure 2d).

Trypan blue staining was used to visualize host cell death over time during the *Eam*-mediated HR. On TRV::*gfp* expressing plants, *Eam*-mediated cell death was clearly visible by 18 hpi (Figure 2e). However, on plants harbouring TRV::*NbCathB-1*, *Eam*-mediated cell death was no higher than background cell death in plants infiltrated with buffer alone, even at 24 hpi (Figure 2e). Significantly, these results demonstrate that non-host HR is suppressed by silencing *NbCathB*.

VIGS and inhibitors suppress an early E. amylovora*-mediated increase in cathepsin B activity*

Real time RT-PCR was used to quantify *NbCathB* expression prior to and after infiltration of *Eam*, and to investigate expression of this gene following VIGS. In non-TRV-inoculated *N. benthamiana*, infiltration of *Eam* led to a modest but significant increase in expression of *NbCathB* at 6 hpi (Figure 3a). Similarly, upregulation of *NbCathB* was observed at 6 hpi with *Eam* in TRV::*gfp* control plants. These results agree with the previous observation (Avrova *et al.*, 2004) that cathepsin B is induced during the HR. In plants inoculated with TRV::*NbCathB-1* the level of expression of *NbCathB* was 10-fold lower than in TRV::*gfp* plants throughout the time course after *Eam* infiltration (Figure 3a).

A colorimetric substrate specific for mammalian cathepsin B was used to assay activity of cathepsin B during the HR. In plants inoculated with TRV::*gfp* an increase in cathepsin B activity was detected at 6 hpi (Figure 3b), mirroring the induction of gene expression witnessed using real-time RT-PCR (Figure 3a). In contrast, no such increase in activity was observed at 12 or 18 hpi (results not shown). A significant decrease in activity was observed in plants inoculated with TRV::*NbCathB-1*, and this activity showed only a negligible increase at 6 hpi with *Eam* (Figure 3b). The modest reduction in activity observed in TRV::*NbCathB-1*-inoculated plants

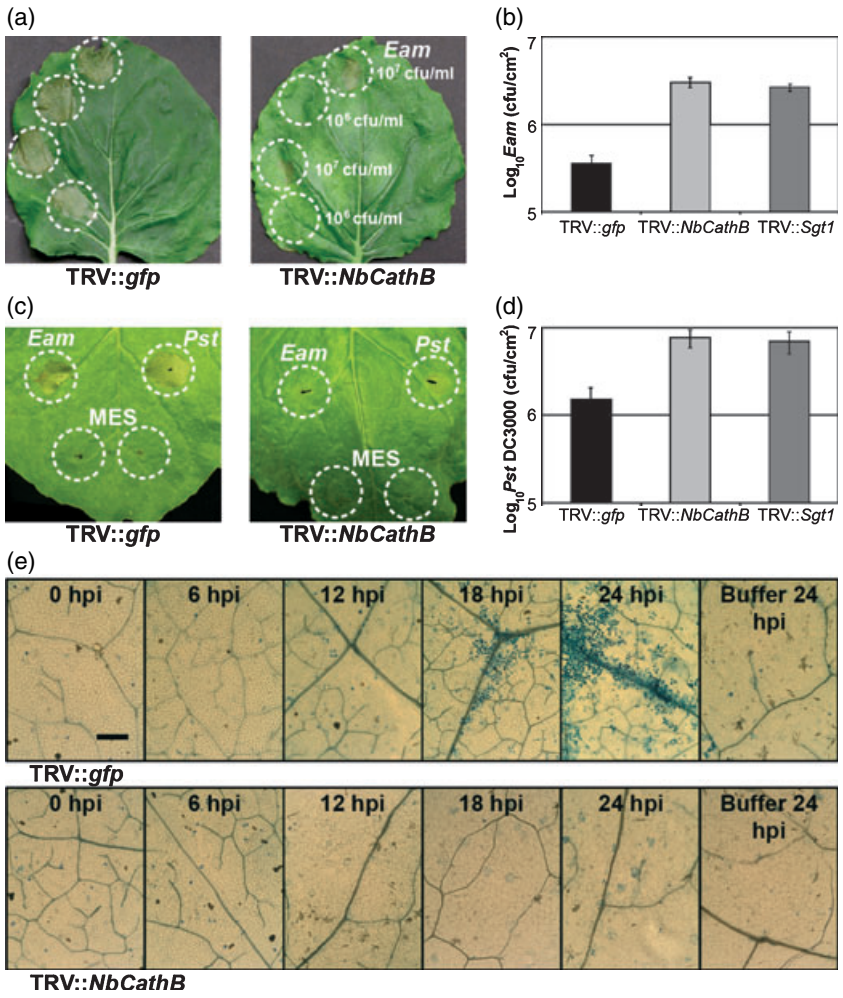

Figure 2. Cathepsin B plays a role in plant non-host disease resistance.
(a) The hypersensitive response (HR) caused by infiltration of 10^6 or 10^7 colony-forming units (cfu) ml^{-1} of *Erwinia amylovora* (*Eam*) onto plants infected with TRV::*gfp* was suppressed on plants infected with TRV::*NbCathB-1*.
(b) Colony counts (cfu cm^{-2}) of viable *Eam* at 4 days post-inoculation in TRV::*gfp*, TRV::*NbCathB-1* or TRV::*Nbsgt1* plants.
(c) The HR caused by infiltration of 10^6 cfu ml^{-1} of *Pseudomonas syringae* pv. tomato (*Pst*) onto plants infected with TRV::*gfp* is suppressed on plants infected with TRV::*NbCathB-1*. No HR was caused by infiltration of 2-(*N*-morpholine)-ethanesulphonic acid, the salt in which the bacteria are suspended.
(d) Colony counts (cfu cm^{-2}) of viable *Pst* at 4 days post-inoculation in TRV::*gfp*, TRV::*NbCathB-1* or TRV::*Nbsgt1* plants. In all cases, experiments involved six replicate plants and were repeated three times with similar results. Colony counts in (b) and (d) are the mean ± SEM of three replicate experiments. Zones of infiltration are indicated by dotted circles.
(e) Detail of leaves stained with trypan blue across a time course [0–24 h post-inoculation (hpi)] after infiltration of 10^6 cfu ml^{-1} *Eam* in plants harbouring TRV::*gfp* (upper panels) or TRV::*NbCathB-1* (lower panels). Bar = 500 μm (for all images).

may be due to this assay detecting other plant protease activities in addition to cathepsin B, and further work will be required to assess the potential range of such specificity. The *Eam*-dependent increase in protease activity at 6 hpi was also observed in non-TRV-inoculated plants and this was suppressed by the inhibitors z-FA-fmk and Ac-LVK-cho (Figure 3c), which were shown to inhibit cathepsin B, amongst other papain activities, in Figure 1(c). These results demonstrate that a rapid, transient *Eam*-mediated increase in cathepsin B transcription is accompanied by an increase in protease activity at 6 hpi in *N. benthamiana*, prior to HR symptoms visualized by trypan blue staining (Figure 2e). Both transcription and activity are considerably reduced in *NbCathB*-silenced plants in which such symptoms are suppressed.

Induction of the HR marker gene Hsr203 is suppressed by cathepsin B silencing

The gene *HSR203* (Pontier *et al.*, 1999) is regarded as a marker of the HR induced by a range of stimuli, including avirulent bacteria. We investigated expression of this gene after infiltration of *Eam* onto plants infected with TRV::*gfp*, TRV::*NbCathB-1* or TRV::*NbCathB-2*. *HSR203* was upregulated moderately in all cases at 12 hpi with *Eam*. By 24 hpi, this gene was upregulated approximately 20-fold in plants inoculated with TRV::*gfp*. However, regardless of the construct used for silencing *NbCathB* expression, *HSR203* expression was suppressed relative to that in TRV::*gfp* plants by approximately 70% in three cases and by approximately 30% in the fourth case (Figure 4). These results are in line with an observed reduction in *Eam*-induced cell death shown in Figure 2(e).

Cathepsin B is involved in a HR triggered by the R3a-Avr3a gene-for-gene interaction

We used VIGS to investigate the role of cathepsin B in the HRs triggered by two gene-for-gene interactions. Recently, we showed that *P. infestans* AVR3a is detected by potato R3a in the host cytoplasm following *Agrobacterium tumefaciens*-mediated transient co-expression of *Avr3a* and *R3a* in

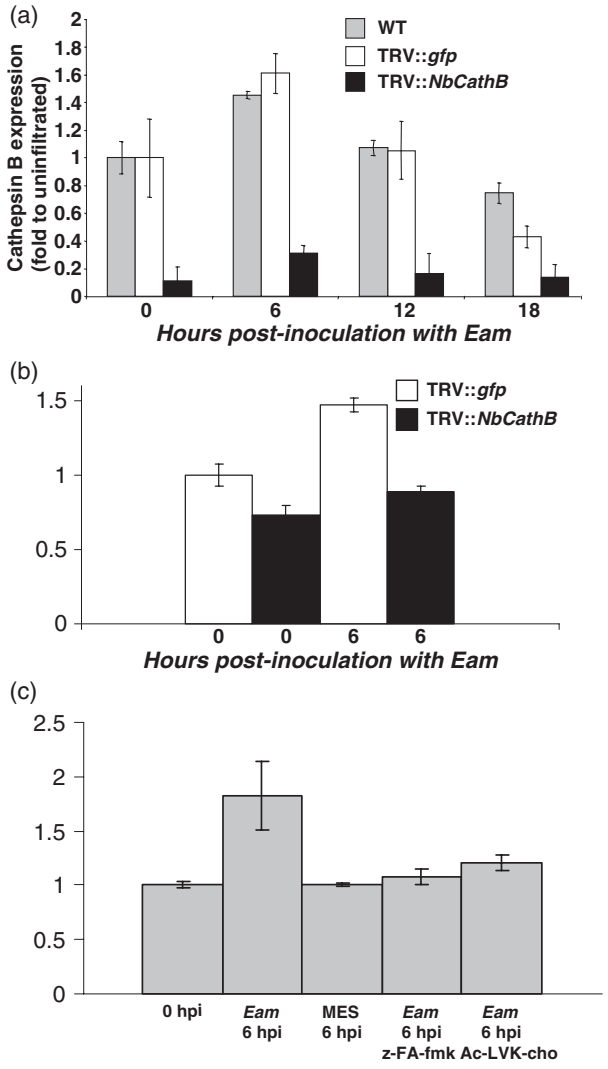

Figure 3. Cathepsin B transcription and activity are upregulated by *Erwinia amylovora* (*Eam*) at 6 h post-inoculation (hpi).
(a) Relative expression of *NbCathB* in uninoculated (WT) and inoculated (TRV::*gfp* or TRV::*NbCathB-1*) *Nicotiana benthamiana* leaves that were untreated (0), or at 6, 12 and 18 hpi with *Eam*. Expression in uninoculated or TRV::*gfp* plants following treatment with *Eam* was compared with the equivalent untreated plants, which was assigned a value of 1.0. Expression in TRV::*NbCathB-1* inoculated plants was relative to expression in untreated TRV::*gfp* plants.
(b) Cathepsin B activity in *N. benthamiana* leaves inoculated with TRV::*gfp* or TRV::*NbCathB-1* that were untreated (0), or at 6 hpi with *Eam*. Activity in TRV::*gfp* plants not treated with *Eam* was assigned a value of 1.
(c) Cathepsin B activity in uninfiltrated *N. benthamiana* leaves (0; assigned a value of 1), and in leaves 6 hpi with *Eam*, with only the buffer in which *Eam* was suspended [2-(*N*-morpholine)-ethanesulphonic acid, MES] or with *Eam* containing 1 mM z-FA-fmk or Ac-LVK-cho. Results in (a)–(c) are each the mean ± SEM of three independent experiments each involving six replicate plants.

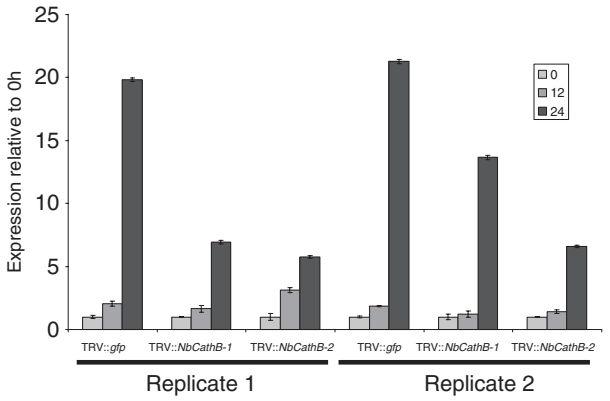

Figure 4. Induction of hypersensitive response marker gene *HSR203* is suppressed by virus-induced gene sampling of *NbCathB*.
Hsr203 gene expression at 0, 12 and 24 hpi with *Erwinia amylovora* (*Eam*) in two replicates, in plants inoculated with TRV::*gfp*, TRV::*NbCathB-1* and TRV::*NbCathB-2*.

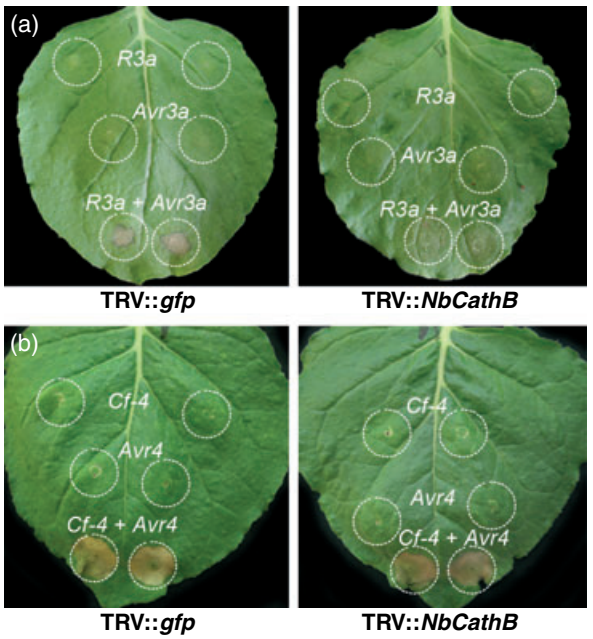

Figure 5. Cathepsin B plays a role in gene-for-gene disease resistance.
(a) The hypersensitive response (HR) caused by co-expression of potato *R3a* and *Phytophthora infestans Avr3a* on plants infected with TRV::*gfp* was suppressed on plants infected with TRV::*NbCathB-1*. No HR was elicited on either plant by expression of *R3a* or *Avr3a* alone.
(b) The HR caused by co-expression of tomato *Cf-4* and *Cladosporium fulvum Avr-4* on plants infected with TRV::*gfp* was not suppressed on plants infected with TRV::*NbCathB-1*. Zones of infiltration are indicated by dotted circles.

N. benthamiana (Armstrong *et al.*, 2005). The HR triggered by interaction of these proteins in plants harbouring TRV::*gfp* was compromised in plants inoculated with either TRV::*NbCathB-1* (Figure 5a) or TRV::*Nbsgt1* (results not shown; demonstrated recently by Bos *et al.*, 2006). These results show that the HR triggered by the cytoplasmic AVR3a-R3a interaction is dependent on both cathepsin B and SGT1.

We investigated the involvement of cathepsin B in the apoplastic gene-for-gene interaction between the products of *C. fulvum Avr4* and tomato *Cf-4*, following their

co-expression in *N. benthamiana* (Van der Hoorn *et al.*, 2000). In this case, whereas silencing of *Nbsgt1* suppressed the HR (results not shown; demonstrated recently by Gabriels *et al.*, 2006), VIGS of *NbCathB* had no effect on the Avr4-Cf-4-mediated HR (Figure 5b), indicating either that not all PCD triggered during disease resistance is dependent on cathepsin B, or that the reduction in cathepsin B levels following VIGS was insufficient to affect cell death triggered by Avr4-Cf4.

Cathepsin B is activated upon secretion into the apoplast

The programme SignalP predicts that the NbCathB protein possesses a signal peptide for extracellular targeting (Supplementary Figure S1a). Using a signal sequence trap strategy, Hugot *et al.* (2004) identified a number of tobacco proteins, including cathepsin B, which appeared to be secreted at late developmental stages. These stages were also associated with increased resistance to *Phytophthora parasitica*. To obtain more evidence that cathepsin B is secreted and active in the apoplast, full-length *NbCathB* (encoding pre-proenzyme) was fused to *mRFP*, encoding a fluorescent marker that is stable in the apoplast. Expression of the NbCathB::mRFP fusion in *N. benthamiana* leaf epidermal cells resulted in largely apoplastic fluorescence (Figure 6a). This was confirmed by co-expression of the construct with a plasma membrane marker EGFP-LT16b (Kurup *et al.*, 2005), with clear mRFP fluorescence detected outside the cell membrane (Figure 6b). Furthermore, treatment with brefeldin A (BFA), an inhibitor of secretion, resulted in retention of mRFP fluorescence within the cell (Figure 6c). Similar BFA treatment of plants over-expressing mRFP fused to a signal peptide for secretion also resulted in retention of the sec::mRFP within the plant cell (Supplementary Figure S4).

To confirm that the mRFP was fused to cathepsin B, a Western blot of total protein extracted from leaves over-expressing either NbCathB::mRFP or sec::mRFP, with or without BFA treatment, was probed with mRFP antibody. A protein of approximately 69 kDa was specifically detected in the NbCathB::mRFP over-expressing material, a size expected of the unprocessed protease, i.e. retaining the signal peptide and prodomain. In independent experiments, the concentration of this protein was considerably greater when secretion was inhibited by BFA treatment (Figure 6d). In contrast, a protein of the size of free mRFP (approximately 30 kDa) was also detected, and this was reduced in concentration upon BFA treatment (Figure 6d), suggesting that the fluorescent tag was cleaved from NbCathB upon secretion. Activity profiling of these protein samples was performed using DCG04, and biotinylated proteins were separated on a protein gel, revealing a range of papain protease activities from 25 to 38 kDa (Figure 6d). Crucially, no activity was detected from the full-length NbCathB::mRFP. These results demonstrate that the NbCathB::mRFP fusion is inactive and is cleaved upon secretion.

Apoplastic proteins were extracted from control *N. benthamiana* leaves and from leaves over-expressing the NbCathB::mRFP fusion and visualized on a polyacrylamide gel. A band of approximately 30 kDa was observed specifically in the NbCathB::mRFP over-expressing material (Figure 6e), less than half the size of the fusion protein. Western hybridization with a mRFP antibody revealed the band to contain free mRFP (Figure 6e). Nevertheless, as free mRFP and activated NbCathB (lacking the signal peptide and prodomain) are predicted to be of similar size, and would thus co-migrate on the gel, the band was excised and analysed by tandem mass spectrometry (MS/MS) and revealed the presence of mRFP and NbCathB (Supplementary Figure S5a), indicating that mRFP had been cleaved from NbCathB to generate two products of similar size.

Activity profiling of apoplastic protein from both control and over-expressing leaf material was performed using DCG-04 and biotinylated proteins were separated on a protein gel, revealing a single band of approximately 30 kDa specifically in the over-expressing sample (Figure 6f). This band was excised and analysed by MS/MS, and the identities of four peptides revealed it to be NbCathB (Supplementary Figure S5b). These peptides all correspond to the protease domain and do not contain the active site cysteine, consistent with the expectation that the prodomain is removed and the active site peptide is biotinylated. Cathepsin B activity was assayed in apoplastic protein from control and NbCathB::mRFP over-expressing leaves using the colorimetric substrate specific for mammalian cathepsin B. This revealed that whereas cathepsin B levels in control, non-pathogen-challenged samples were similar to those shown earlier (Figure 3b), cathepsin B activity more than six-fold higher was observed in the over-expressing plants (Figure 6g). This confirmed the efficacy of this assay in determining plant cathepsin B activity. Furthermore, the activity was inhibited by use of the cathepsin B inhibitor Ac-LVK-cho and the papain inhibitor E64 (Figure 6h). Taken together, the results indicate that NbCathB is secreted and is activated only upon secretion.

To confirm that secretion of active NbCathB was not an artefact of over-expression in *N. benthamiana*, we performed large-scale protease activity profiling on apoplastic proteins of the closely related tomato. Tomato was used because apoplastic papain proteases were difficult to detect in *N. benthamiana* (Figure 6g), whereas apoplastic proteins can be obtained effectively from tomato (Krüger *et al.*, 2002). Tomato leaves were vacuum-infiltrated with DCG-04, incubated, and apoplastic fluids were carefully isolated. Biotinylated proteins were separated on a protein gel and the 30 kDa region (Figure 7) was excised and analysed by MS/MS. This revealed the presence of two tomato cathepsin B-like proteases (TC175119 and TC182010) represented with seven

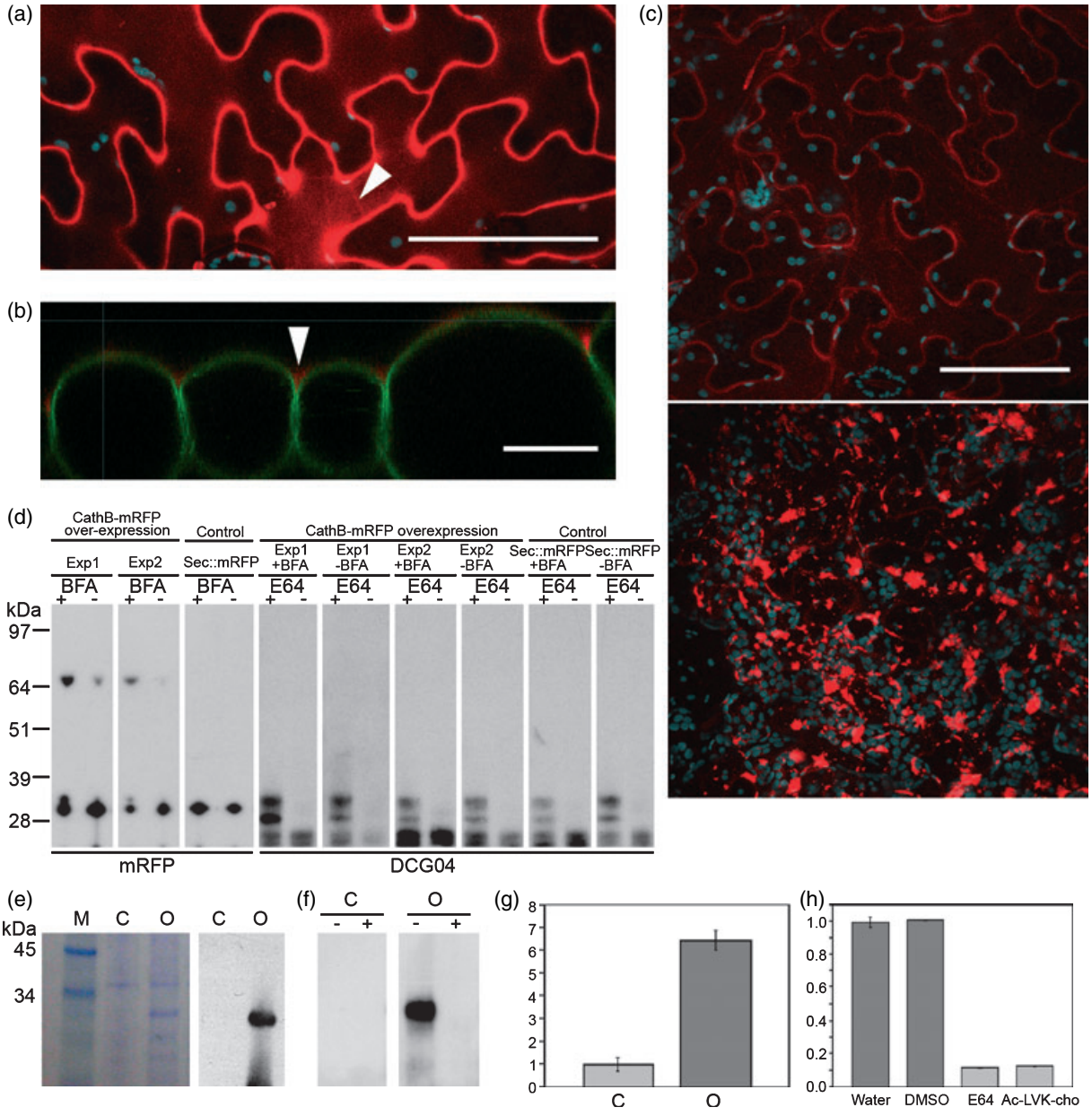

and six peptides, respectively (Supplementary Figure S5c). A phylogenetic tree constructed following alignment of these sequences with *NbCathB* and cathepsin B sequences from potato and tobacco revealed that *NbCathB* is likely to be the orthologue of tomato sequence TC182010 (Supplementary Figure S1b). These data demonstrate that cathepsin B is a secreted, active protease in the tomato apoplast.

Discussion

Inhibitors have been used to implicate a diverse range of plant proteases in pathogen perception and in subsequent signalling and execution of disease resistance. They have been utilized to demonstrate roles for caspases in regulation and execution of plant PCD such as that characterizing the HR (Van der Hoorn and Jones, 2004; Woltering, 2004). In contrast, the tomato papain protease RCR3 plays a role in pathogen perception by recognition of AVR2 from *C. fulvum*, and recognition can be prevented by the general papain inhibitor E64 (Rooney *et al.*, 2005). E64 has also been shown to prevent the HR whilst not affecting caspase activities, implying the involvement of papain proteases in PCD (D'Silva *et al.*, 1998; Coffeen and Wolpert, 2004; Woltering, 2004). However, the identities of papain proteases involved in regulation or execution of the HR have proven elusive. Here, we used cathepsin B inhibitors to provide evidence of a role for this papain

Figure 6. Cathepsin B is activated upon secretion.
(a) Expression of the NbCathB::mRFP (monomeric red fluorescent protein) fusion in leaf epidermal cells resulted in largely apoplastic fluorescence; this image is a maximum projection of a stack of 20 confocal images covering 19 μm in depth. In highly over-expressing cells some fluorescence visible within the cell (arrowhead) appeared to be in the endoplasmic reticulum. Scale bar is 100 μm.
(b) When co-expressed with the plasma membrane marker EGFP-LT16b, NbCathB::mRFP fluorescence was observed outside the GFP-LT16b-labelled plasma membrane of the abaxial epidermal cells. This image is a cross-section through a projected stack of 72 confocal images covering 43 μm in depth. mRFP fluorescence was particularly bright close to cell junctions (arrowhead). Scale bar is 20 μm.
(c) Apoplastic localization of NbCathB::mRFP is retained following treatment with water for 6 h (upper panel) but the protein formed aggregates within the cell (lower panel) when leaves were treated with brefeldin A (BFA), which inhibits secretion. Scale bar is 50 μm.
(d) Western blot of total protein from plants over-expressing NbCathB::mRFP (from two independent experiments) or secreted mRFP (sec:mRFP), with or without BFA treatment, probed with mRFP antibody (first three panels). Protease activity profiling of total protein from plants over-expressing NbCathB::mRFP or sec::mRFP (control), with (+) or without (–) BFA treatment, using a biotinylated derivative of E-64 (DCG-04) in the presence (+) or absence (–) of 0.4 mM inhibitor E–64.
(e) Left panel shows a protein gel of apoplastic protein from control (C) and NbCathB::mRFP over-expressing (O) *Nicotiana benthamiana*, indicating a specific band of approximately 30 kDa specific to the 'O' sample. Tandem mass spectrometry (MS/MS) analysis of this band identified peptides from both NbCathB and mRFP (Supplementary Figure S5a). The right panel indicates western hybridization of anti-mRFP antibody to the protein gel shown in the left panel.
(f) Activity profiling of apoplastic protein from control (C) and NbCathB::mRFP over-expressing (O) plants using biotinylated derivative of E-64 (DCG-04) in the presence (+) or absence (–) of 0.4 mM inhibitor E-64. The MS/MS analysis of the 30 kDa band specific to the O sample identified peptides from NbCathB (Supplementary Figure S5b).
(g) Cathepsin B activity was more than six-fold higher in apoplastic protein from NbCathB::mRFP-over-expressing (O) plants than from control (C) plants (set at a value of 1 on the *y*-axis).
(h) Cathepsin B activity in apoplastic protein from NbCathB::mRFP-over-expressing plants was inhibited approximately 90% by papain inhibitor E64 and by cathepsin B inhibitor Ac-LVK-cho (compared to water or DMSO treatments). Results in (g) and (h) are each the mean ± SEM of two independent experiments.

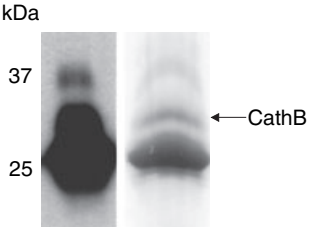

Figure 7. Apoplastic localization of cathepsin B in tomato.
Biotinylated proteins isolated from tomato apoplast after DCG-04 labelling, detected with streptavidin-horseradish peroxidase (left) and colloidal Coomassie stain (right) and cathepsin B was identified by tandem mass spectroscopy analysis (Supplementary Figure S5c).

protease in *N. benthamiana* non-host disease resistance to *E. amylovora*. However, the inhibitors, whilst suppressing cathepsin B activity, also suppressed additional papain proteases and VIGS was required to demonstrate unequivocal involvement of cathepsin B not only in non-host disease resistance but also in the HR triggered by interaction of potato *R3a* and *P. infestans Avr3a* gene products.

Based on the similarities between three cathepsin B genes in *A. thaliana* and multiple EST sequence contigs in potato, cathepsin B is encoded by a family of closely related genes in plants and, in this work, VIGS involved constructs that were likely to silence the entire cathepsin B family in *N. benthamiana.* Further work will be needed to ascertain whether independent cathepsin B genes play different roles in plant development or in disease resistance. The reduction of disease resistance to *Eam* and *Pst* following silencing of *NbCathB* resulted in a five- to eight-fold increase in viable bacterial cells, similar to those seen when silencing *Nbsgt1* (Figure 2). Moreover, as VIGS of *NbCathB* suppressed the HR triggered by co-expression of *R3a* and *Avr3a*, we conclude that cathepsin B is involved in both host and non-host disease resistance. SGT1 also plays a role in both forms of disease resistance, but not in all cases (Peart *et al.*, 2002; Muskett and Parker, 2003). Similarly, as cathepsin B was not required for Cf4-AVR4-mediated HR, it also is not involved in all types of gene-for-gene disease resistance. Intriguingly, SGT1 was required for CF4-AVR4-mediated HR (Gabriels *et al.*, 2006; and this study), indicating overlapping but operationally distinct roles for these proteins in disease resistance.

In animals, cathepsin B can function as a regulator of PCD following its relocalization from the lysosome to the cytosol (Kingham and Pocock, 2001; Vancompernolle *et al.*, 1998; Guicciardi *et al.*, 2001; Zeiss, 2003). Here, VIGS of *NbCathB* suppressed PCD triggered by co-expression of AVR3a and R3a, and by infiltration of *Eam*, as visualized using trypan blue staining and suppression of the HR marker gene *Hsr203*. It is thus reasonable to speculate that cathepsin B also plays a role in regulation of PCD in plants. Nevertheless, we provided evidence that cathepsin B may not be required for all forms of PCD in plants. This is perhaps unsurprising as morphologically distinct forms of PCD suggest more than one genetically programmed route for the death of plant cells (van Doorn and Woltering, 2005). Indeed, there is more than one form of PCD in animals with varying dependence on different classes of protease (Podgorski and Sloane, 2003; Zeiss, 2003).

Apoptosis in animals is characterized by the tightly regulated activation of numerous constitutively expressed protease proenzymes, as is the case for caspases, or by the cellular relocalization of proteases such as cathepsin B (Podgorski and Sloane, 2003). The recently described plant saspases represent a class of PCD-associated proteases that are constitutively active and relocalized to the apoplast upon PCD induction (Coffeen and Wolpert, 2004). Nevertheless, *VPE*, encoding a protease with caspase-1-like activity, is

induced at the transcriptional level during the HR (Hatsugai *et al.*, 2004), revealing a difference in the induction of PCD in animals and plants. Cathepsin B represents a further protease that is constitutively expressed in animals but transcriptionally upregulated in plants during processes involving PCD in response to pathogen attack (this study and Avrova *et al.*, 2004). Indeed, cathepsin B is also induced during senescence, a process also involving PCD in plants (Gepstein *et al.*, 2003; Bhalerao *et al.*, 2003).

Many plant defence-associated proteases are secreted into the apoplast, including RCR3 (Krüger *et al.*, 2002), P69B (Tornero *et al.*, 1996), CDR1 (Xia *et al.*, 2004) and saspases (Coffeen and Wolpert, 2004). The saspases represent one of three distinct proteolytic activities responsible for victorin-mediated PCD, the others being a different caspase-like activity and a papain-like activity. Coffeen and Wolpert (2004) provided evidence that these activities were components of a signal cascade responsible for victorin- and heat-mediated PCD, and they postulated that saspase was upstream of other proteases within this signalling process, and possibly involved in their activation. It is thus interesting that cathepsin B is also secreted into the apoplast and is activated upon secretion; its potential interaction with other proteases warrants detailed investigation.

Despite cathepsin B being secreted, VIGS of cathepsin B compromised the HR triggered by intracellular recognition of AVR3a and R3a. Similar observations have been made with the extracellular cathepsin D-like protein CDR1. Antisense suppression of *CDR1* compromised the HR triggered by the intracellular recognition of *P. syringae* AvrRpm1, by mediation of an unidentified cell-to-cell peptide signalling system (Xia *et al.*, 2004). It has thus been established that, in plants, extracellular proteases can regulate the HR following intracellular recognition of pathogen effector proteins.

The presence of so many defence-associated proteases in the plant extracellular fluid highlights the potential importance of protease inhibitors secreted into the apoplast by invading pathogens in the establishment of infection (Tian *et al.*, 2004; Rooney *et al.*, 2005). The proteolytic battle for resistance or susceptibility outside the plant cell promises to be a fascinating area of study in the coming years.

Experimental procedures

Bacterial inoculations, disease resistance and cell death measurement

Erwinia amylovora (*Eam*) strain 1430 was cultured in King's broth supplemented with 6 mM $MgSO_4$ incubated at 30°C and 100 ***g*** over night. Bacteria were resuspended in sterile 5 mM 2-(*N*- morpholine)-ethanesulphonic acid (MES). *Eam* suspensions (10^6 cfu ml^{-1}) in 5 mM MES were pressure infiltrated with or without 1 mM inhibitors (cathepsin B, S and L inhibitor, Z-FGNHO-Bz; cathepsin B inhibitors z-FA-fmk, Ac-LVK-cho and CA-074 Me) (Calbiochem®, Merck Biosciences; http://www.merckbiosciences.com/) into three leaves on each of six wild-type *N. benthamiana* plants. For VIGS experiments, 10^7 or 10^6 cfu ml^{-1} *Eam* and 10^6 cfu ml^{-1} *Pst* DC3000 were infiltrated into *N. benthamiana* plants inoculated with TRV::*gfp*, TRV::*sgt1* or TRV::*NbCathB* as described previously (Cao *et al.*, 1994).

For viable *Eam* and *Pst* colony counting experiments, leaves were harvested 4 dpi. Whole leaves or leaf segments of equivalent size were ground in 1 ml of 10 mM $MgCl_2$ using micropestles. Four subsequent serial dilutions of 100 μl sample in 900 μl of 10 mM $MgCl_2$ were performed and 100 μl of the 10^{-4} dilution spread on King's Broth (KB) plates containing 50 mg l^{-1} rifampicin and incubated at 30°C for 48 h. Trypan blue stain, used to visualize host cells dying in response to *Eam*, was performed as described (Tissier *et al.*, 1999).

Avr3a-R3a *and* Cf-4-Avr-4 *co-expression*

Avr3a-R3a co-expression was performed as described (Armstrong *et al.*, 2005), except that the infiltration buffer was the same as for inhibitor infiltrations. The AGL0 strain carrying pBINplus::*R3a* was resuspended to OD_{600} = 1, and mixed in a 1:1 ratio with OD_{600} = 0.4 suspension of LB4404 carrying pGR106::*Avr3a* for co-inoculation. Photographs were taken after HR symptoms developed at 6 dpi. Co-expression of *C. fulvum Avr4* and tomato *Cf-4* was as described previously (Van der Hoorn *et al.*, 2000).

Cathepsin B activity

Frozen leaves were finely ground, 300 μl of extraction buffer (50 mM monobasic, 50 mM dibasic potassium phosphate, pH 6.8 and 1 mM DTT) was added and the tissue homogenized. Protein samples were incubated on ice for 15 min and spun at maximum speed (16 000 ***g***) for 15 min to pellet cell debris. Supernatant was kept on ice or frozen at −70°C. Assays were performed using clear 96-well microtitre plates (Fisher Scientific, http://www.fisher.co.uk/) and a DIAS plate reader (Dynatech Laboratories; http://www.dynatechlaboratories.com).

Bradford reagent (Bio-Rad; http://www.bio-rad.com/) was diluted 1:5 with sterile distilled water (SDW), aliquoted (199 μl) to each well of a 96-well microtitre plate and 1 μl of protein extract was added and mixed. The reaction was left for 30 min at room temperature (21°C) .and optical density was measured at 595 nm. The protein concentration was calculated using a formula derived from a bovine serum albumin dilution series ranging from 0 to 6 μg.

Cathepsin B colorimetric substrate Z-Arg-Arg-*p*NA, 2HCl (Calbiochem®, Merck Biosciences) was diluted to 1 mM in SDW. Assay buffer was prepared as recommended by Calbiochem®. Assay buffer and colorimetric substrate were mixed in equal volumes, then mixed with 1.8× volume of SDW. One hundred and forty microlitres of buffer/substrate solution was aliquotted into each well of a 96-well microtitre plate and 10 μl of protein extract added, mixed and incubated at room temperature for 30 min. Optical density was read at 405 nm using a DIAS plate reader. Protein activity was divided by total protein (mg ml^{-1}) in crude extracts calculated using a Bradford assay, reading the optical density at 595 nm.

Cloning of NbCathB

The *N. benthamiana NbCathB* gene was obtained by aligning cathepsin B DNA sequences from *S. tuberosum* (accession number AY450641) and *N. rustica* (X81995). Primers (cathB-F 5′-TTT GGGTACCTAAGCGCCTTCTTG-3′ and cathB-R 5′-TTTTCCATGGG TAAGGATCACACTCTTC-3′) designed to anneal to common sequences were used to PCR amplify the equivalent sequence from

N. benthamiana cDNA. The full-length coding region for *NbcathB* was obtained through 3′-rapid amplification of cDNA ends (RACE) according to specifications in the SMART RACE II kit (BD Clontech; http://www.clontech.com/). The forward primer cathB-F, for cloning into the VIGS vector, was used as the gene-specific primer in conjunction with the 3′-RACE primers from the kit. Sequencing and BLAST results indicated that the fragment had 97% homology at the nt level to the *N. rustica* cathepsin B-like cysteine protease mRNA (Not shown). Therefore, a primer to amplify the *N. benthamiana* fragment from the start codon was designed from the *N. rustica* sequence and used (CATHSTARTa: 5′-GGCACGAGGCCAAATAT G-3′) in conjunction with the 3′- RACE primer. The resulting 1400-bp amplification product was cloned into pGEM-T EASY (Promega; http://www.promega.com/) according to the manufacturer's specifications and sequenced using the Applied Biosystems Bigdye® v3.1 Terminator sequencing kit (http:http://www.appliedbiosystems.com/). The *NbCathB* accession number is DQ492287.

Phylogenetic analyses of cathepsin B sequences

The 13 cathepsin B nt sequences used for the tree in Supplementary Figure S1(b) [DQ492287 from *N. benthamiana;* AF359422 from *Nicotiana tabacum*; TC137447, TC145097, TC152070 and TC142279 from potato; TC175119 and TC182010 from tomato; NM_100110 (At1 g02300); NM_100111 (At1 g02305); NM_116392 (At4 g01610) and the splice variant of NM_178950 from *A. thaliana*; and NM_001908 from *H. sapiens*] were used to obtain a back-translated alignment of their source nt sequences, using an *ad hoc* Python script that matched the protein sequence to the coding sequence fragments in the source nt sequence. This script first reduced the EST sequences to their coding sequences, and these were threaded onto the full protein sequence alignment, using t_coffee, with the protocol: t_coffee -other_pg seq_reformat -in cathB_backtrans.fas \ -in2 cathB_prot.fasta_aln -action +thread_dna_on_prot_aln -output phylip_aln. This alignment was cropped to only those regions shared by all sequences. The seqboot package was used to generate 1000 bootstrap sequences from this truncated alignment. The PHYLIP package dnaml was used to generate maximum-likelihood trees. Trees were generated based on a single alignment, and on 1000 bootstrap alignments generated from these sequences.

Plant material and VIGS constructs

Virus-induced gene silencing experiments were conducted in containment glasshouses under Scottish Executive Environment and Rural Affairs Department licenses GM/203/2004 and GM/210/2004. Growth of *N. benthamiana* and use of a Tobacco rattle virus vector (TRV-2b) for VIGS was as described previously (Valentine *et al.*, 2004). Primer sequences used to clone a 364-bp portion of *NbCathB* into TRV were cathB-F, 5′-TTTGGGTACCTAAGCGCCTTCTTG-3′, and cathB-R, 5′-TTTTCCATGGGTAAGGATCACACTCTTC-3′. The *NbCathB* PCR product was subcloned into pGEM-T EASY then excised by *Nco*I–*Not*I digestion and subcloned in antisense orientation into *Nco*I–*Eag*I-digested TRV vector to generate TRV::*NbCathB-1*. The insert was also cloned into the TRV binary vector pBinTRV2b (Liu *et al.*, 2002). Silencing with this construct produced similar results to the TRV::*NbCathB-1* construct described above. An independent 247-bp fragment of *NbCathB* (see Supplementary Figure S1a) was cloned into pBinTRV2b by utilizing the primers cathB2-F, 5′-AATTGAATTCGAGAGGACTATTGGCTTC TTGC-3′, and cathB2-R, 5′-AAAAGTTAACTTGTTCCCCAGTCTTCAG AGA-3′. This *NbCathB* PCR product was subcloned into pGEM-T EASY, excised by *Eco*RI and *Hpa*I and cloned in antisense orientation into *Eco*RI- and *Hpa*I-digested binary vector pBinTRV2b to generate TRV::*NbCathB-2.* Primers for cloning a 580-bp portion of *Nbsgt1* (accession number AF494083.1) were 5′-TTTTGGTAC CTTCGCCGACCGTG-3′ and 5′-TATTCCATGGGCAGGTGTTATCTT C-3′. The PCR product was subcloned into pGEM-T EASY. Following *Avr*II digestion and blunting using T4 DNA polymerase (New England Biolabs; http://www.neb.com/), *Nbsgt1* cDNA was excised by *Not*I digestion and subcloned in antisense orientation into TRV (linearized by *Hpa*I and *Eag*I) to generate TRV::*Nbsgt1*. TRV::*gfp* (Valentine *et al.*, 2004) was used as a control of TRV infection.

Real time RT-PCR

Total RNA extraction and first-strand cDNA synthesis using random hexamer primers were as described previously (Lacomme *et al.*, 2003). For SYBR green-based real-time RT-PCR (QuantiTect SYBR GreenPCR kit, Qiagen; http://www.qiagen.com/) experiments, primer pairs were designed outside the region of cDNA targeted for silencing using PRIMER EXPRESS software supplied with the ABI PRISM 7700 Sequence Detection System (Applied Biosystems) following the manufacturer's guidelines. Expression of *NbCathB* and *NbHsr203* were assessed relative to that of 26S rRNA. The primers for 26S rRNA were 5′-CACGGACCAAGGAGTCTGACAT-3′ and 5′-TCCCACCAATCAGCTTCCTTAC-3′. Primers for *NbCathB* were designed from *N. benthamiana* accession DQ492287 and were 5′-CAGCTCCGATCCACACAGTA-3′ and 5′-GAGCGAAATCCTCGTAA ACAG-3′. Additional primers (5′-CAGCTCCGATCCACACAGTA-3′ and 5′-GAGCGAAATCCTCGTAAACAG-3′) were used to assess transcription level of *NbCathB* after silencing with TRV::*NbCathB-2*. Primers for *NbHsr203* were designed from *N. tabacum* accession X77136 5′-ATGAAAAGCAAGTGATAGAGGAAGTA-3′ and 5′-GCTC GGCCATGAATTTGAC-3′. Primer concentrations giving the lowest threshold cycle (Ct) value were selected for further analysis. Detection of real-time RT-PCR products, calculations and statistical analysis were performed as previously described (Lacomme *et al.*, 2003).

Western hybridization

For immunodetection of SGT1 and mRFP, protein extraction and Western blot analyses were as previously described (Lacomme and Santa Cruz, 1999). Blots were incubated with primary antibody against SGT1 (rat polyclonal, 1:2000; Takahashi *et al.*, 2003) and for mRFP (rabbit polyclonal, 1:2000). Alkaline phosphatase-conjugated antirat IgG (Sigma; http://www.sigmaaldrich.com/) was used as a secondary antibody for SGT1 for detection in silenced and control plants, and peroxidase-conjugated antirabbit IgG (Sigma) was used for mRFP detection.

Activity profiling experiments.

To investigate specificity of cathepsin B inhibitors, DCG-04 was incubated with Arabidopsis leaf extracts and competed with E-64, z-FA-fmk, Ca-074-Me and Ac-LVK-cho as described previously (Van der Hoorn *et al.*, 2004). After labelling, biotinylated proteins were purified and detected on a protein blot using streptavidin-HRP, as described previously (Van der Hoorn *et al.*, 2004).

To investigate apoplastic cathepsin B activity, 186 leaflets of tomato cultivar MoneyMaker were vacuum infiltrated with 2 mg l^{-1} DCG-04 and 10 mg l^{-1} L-cysteine and incubated for 5 h at room-temperature. Apoplastic fluids were subsequently isolated from ice-cooled leaflets (Krüger *et al.*, 2002) and biotinylated proteins were captured as

described previously (Van der Hoorn *et al.*, 2004). Isolated proteins were separated on a 10% SDS polyacrylamide gel and stained with colloidal Coomassie. The 30-kDa protein band was excised from the gel, treated with trypsin, and eluted peptides were analysed by MS/MS as described previously (Van der Hoorn *et al.*, 2004).

Confocal microscopy of cathepsin B localization

NbCathB cDNA was PCR amplified and cloned into pGEM-T vector (Promega). The coding region was PCR amplified from a sequence-confirmed clone using primers designed to introduce an *Asc*I site at the 5′ end and a *Not*I site at the 3′ end while removing the stop codon. This PCR fragment was cloned into a version of pENTER 1A (Invitrogen; http://www.invitrogen.com/) modified to contain *Asc*I and *Not*I restriction sites in the multiple cloning region. The *NbCathB* sequence was recombined with a derivative of the Gateway vector pMDC84 (Curtis and Grossniklaus, 2003) in which the mgfp6 coding sequence had been replaced by *mRFP* (Campbell *et al.*, 2002). The cathepsin B–mRFP fusion construct was electroporated into *Agrobacterium tumefaciens* strain LBA4404 and infiltrated into leaves from 4-week-old *N. benthamiana*.

A 1:1 mixture of agrobacteria containing the *EGFP-LT16b* and *cathepsin B-mRFP* constructs was infiltrated as described for *R3a* and *Avr3a* above. Cells expressing fluorescent protein fusions were observed using a Leica TCS-SP2 AOBS confocal microscope (http://www.leica.com/) between 1 and 5 dpi. Images were obtained using an HCX APO 63×/0.9 W water-dipping lens. Monomeric red fluorescent protein was imaged using an excitation wavelength of 568 nm from a 'lime' diode laser with emissions collected between 600 and 630 nm. Green fluorescent protein was imaged using 488-nm excitation from an argon laser, with emissions collected between 500 and 530 nm. Chlorophyll-associated autofluorescence was also obtained after excitation at 488 nm and the emissions collected between 650 and 700 nm. Brefeldin A treatment was with 10 μg ml^{-1} (in water), infiltrated 24 h after agroinfiltration of the cathepsin B-mRFP construct and leaves were observed under the confocal microscope 6 h later.

Acknowledgements

We are grateful to the Scottish Executive Environment and Rural Affairs Department (SEERAD) and the Biotechnology and Biological Sciences Research Council (BBSRC) for funding this work. We thank Professor Pierre de Wit (Department of Phytopthology, Wageningen University) for providing *Cf-4* and *Avr-4* expression constructs, Dr K. Shirasu (Sainsbury Laboratory, Norwich, UK) for providing anti-SGT1 antisera and Professor John Hancock (Institute for Molecular Bioscience, Brisbane, Australia) for anti-mRFP antisera. The binary vector containing plasma membrane marker EGFP-LT16b was provided by Smita Kurup (Rothamsted, UK).

Supplementary material

The following supplementary material is available for this article online:

Figure S1. (a) Alignment of protein sequences of cathepsin B from *Nicotiana benthamiana*, *Nicotiana rustica*, *Solanum tuberosum*, *Arabidopsis thaliana* and *Homo sapiens*.

(b) Maximum likelihood topology generated from cathepsin B nucleotide sequences from *N. benthamiana*, *N. tabacum*, potato, tomato and from *A. thaliana*; and rooted to the outgroup cathepsin B sequence from *H. sapiens.*

Figure S2. (a) Relative expression of *NbCathB* in TRV::*gfp*, TRV::*NbCathB-1* and TRV::*NbCathB-2* infected plants, measured using real-time RT-PCR.

(b) Western blot analysis of SGT1 protein levels in TRV::*gfp* and TRV::*Nbsgt1b* infected plants.

Figure S3. Colony counts (cfu ml^{-1}) of viable *E. amylovora* at 4 days post-inoculation in TRV::*gfp*, TRV::*NbCathB-1* or TRV::*NbCathB-2* plants.

Figure S4. Use of Brefaldin A (BFA) prevents secretion of NbCathB::mRFP and sec::mRFP. Expression of NbCathB::mRFP (a) and sec::mRFP (b) in *Nicotiana benthamiana* leaves results in largely apoplastic fluorescence. However, treatment with BFA resulted in retention of the monomeric red fluorescent protein (mRFP) within the cell for both NbCathB::mRFP (c) and sec::mRFP (d).

Figure S5. Identification of cathepsin B peptides.

(a) Identified peptides from *Nicotiana benthamiana* cathepsin B and monomeric red fluorescent protein (mRFP) in the apoplast following over-expression of *NbCathB::mRFP*.

(b) Identified peptides from active *NbCathB* following over-expression and activity profiling with biotinylated DCG-04.

(c) Identified peptides from tomato cathepsin B-like proteases in the tomato apoplast following tandem mass spectrometry analysis.

This material is available as part of the online article from http://www.blackwell-synergy.com

References

Alfano, J.R. and Collmer, A. (2004) Type III secretion system effector proteins: double agents in bacterial disease and plant defence. *Annu. Rev. Phytopath.* **42**, 385–414.

Armstrong, M.R., Whisson, S.C., Pritchard, L. *et al.* (2005) An ancestral oomycete locus contains late blight avrirulance gene *Avr3a*, encoding a protein that is recognized in the host cytoplasm. *Proc. Natl Acad. Sci. USA*, **102**, 7766–7771.

Avrova, A.O., Taleb, N., Rokka, V.M. *et al.* (2004) Potato oxysterol binding protein and cathepsin B are rapidly up-regulated in independent defence pathways that distinguish *R* gene-mediated and field resistances to *Phytophthora infestans*. *Mol. Plant Pathol.* **5**, 45–56.

Bhalerao, R., Keskitalo, J., Sterky, F. *et al.* (2003) Gene expression in autumn leaves. *Plant Physiol.* **131**, 430–442.

Bos, J.I.B., Kanneganti, T.D., Young, C., Cakir, C., Huitema, E., Win, J., Armstrong, M.R., Birch, P.R.J. and Kamoun, S. (2006) The C-terminal half of *Phytophthora infestans* RXLR effector AVR3a is sufficient to trigger R3a-mediated hypersensitivity and suppress INF1-induced cell death in *Nicotiana benthamiana*. *Plant J.* **48**, 165–176.

Campbell, R.E., Tour, O., Palmer, A.E., Steinbach, P.A., Baird, G.S., Zacharias, D.A. and Tsien, R.Y. (2002) A monomeric red fluorescent protein. *Proc. Natl Acad. Sci. USA*, **99**, 7877–7882.

Cao, H., Bowling, S.A., Gordon, A.S. and Dong, X. (1994) Characterization of an arabidopsis mutant that is nonresponsive to inducers of systemic acquired resistance. *Plant Cell*, **6**, 1583–1592.

Chichkova, N.V., Kim, S.H., Titova, E.S., Kalkum, M., Morozov, V.S., Rubtsov, Y.P., Kalinina, N.O., Taliansky, M.E. and Vartapetian, A.B. (2004) A plant caspase-like protease activated during the hypersensitive response. *Plant Cell*, **16**, 157–171.

Coffeen, W.C. and Wolpert, T.J. (2004) Purification and characterization of serine proteases that exhibit caspase-like activity and are associated with programmed cell death in *Avena sativa*. *Plant Cell*, **16**, 857–873.

Curtis, M.D. and Grossniklaus, U. (2003) A gateway cloning vector set for high-throughput functional analysis of genes *in planta*. *Plant Physiol.* **133**, 462–469.

D'Silva, I., Poirier, G.G. and Heath, M.C. (1998) Activation of cysteine proteases in cowpea during the hypersensitive response – a form of programmed cell death. *Exp. Cell Res.* **245**, 389–399.

Del Pozo, O. and Lam, E. (1998) Caspases and programmed cell death in the hypersensitive response of plants to pathogens. *Curr. Biol.* **8**, 1129–1132.

van Doorn, W.G. and Woltering, E.J. (2005) Many ways to exit? Cell death categories in plants. *Trends Plant Sci.* **10**, 117–122.

Foghsgaard, L., Wissing, D., Mauch, D., Lademann, U., Bastholm, L., Boes, M., Elling, F., Leist, M. and Jaattela, M. (2001) Cathepsin B acts as a dominant execution protease in tumour cell apoptosis induced by tumour necrosis factor. *J. Cell Biol.* **153**, 999–1010.

Gabriels, S.H., Takken, F.L., Vossen, J.H. *et al.* (2006) CDNA-AFLP combined with functional analysis reveals novel genes involved in the hypersensitive response. *Mol. Plant Microbe Interact.* **19**, 567–576.

Gepstein, S., Sabehi, G., Carp, M.J., Hajouj, T., Nesher, M.F., Yariv, I., Dor, C. and Bassani, M. (2003) Large-scale identification of leaf senescence-associated genes. *Plant J.* **36**, 629–642.

Greenberg, J.T. and Yao, N. (2004) The role and regulation of programmed cell death in plant-pathogen interactions. *Cell Microbiol.* **6**, 201–211.

Guicciardi, M.E., Miyoshi, H., Bronk, S.F. and Gores, G.J. (2001) Cathepsin B knockout mice are resistant to tumour necrosis factor-α-mediated hepatocyte apoptosis and liver injury. *Am. J. Pathol.* **159**, 2045–2054.

Hatsugai, N., Kuroyanagi, M., Yamada, K., Meshi, T., Tsuda, S., Kondo, M., Nishimura, M. and Hara-Nishimura, I. (2004) A plant vacuolar protease, VPE, mediates virus-induced hypersensitive cell death. *Science*, **305**, 855–858.

Hugot, K., Riviere, M.P., Moreilhon, C., Dayem, M.A., Cozzitorto, J., Arbiol, G., Barbry, P., Weiss, C. and Galiana, E. (2004) Coordinated regulation of genes for secretion in tobacco at late developmental stages: association with resistance against oomycetes. *Plant Physiol.* **134**, 858–870.

Hye-Sook, O. and Collmer, A. (2005) Basal resistance against bacteria in *Nicotiana benthamiana* leaves is accompanied by reduced vascular staining and suppressed by multiple *Pseudomonas syringae* type III secretion system effector proteins. *Plant J.* **44**, 348–359.

Kingham, P.J. and Pocock, J.M. (2001) Microglial secreted cathepsin B induces neuronal apoptosis. *J. Neurochem.* **76**, 1475–1484.

Krüger, J., Thomas, C.M., Golstein, C., Dixon, M.S., Smoker, M., Tang, S., Mulder, L. and Jones, J.D. (2002) A tomato cysteine protease required for Cf-2-dependent disease resistance and suppression of autonecrosis. *Science*, **296**, 744–747.

Kurup, S., Runions, J., Kohler, U., Laplaze, L., Hodge, S. and Haseloff, J. (2005) Marking cell lineages in living tissues. *Plant J.* **42**, 444–453.

Lacomme, C. and Santa Cruz, S. (1999) Bax-induced cell death in tobacco is similar to the hypersensitive response. *Proc. Natl Acad. Sci. USA*, **96**, 7956–7961.

Lacomme, C., Hrubikova, K. and Hein, I. (2003) Enhancement of virus-induced gene silencing through viral-based production of inverted-repeats. *Plant J.* **34**, 543–553.

Liu, Y., Schiff, M. and Dinesh-Kumar, S.P. (2002) Virus-induced gene silencing in tomato. *The Plant J.* **31**, 777–786.

Muskett, P. and Parker, J. (2003) Role of SGT1 in the regulation of plant R gene signaling. *Microbes Infect.* **5**, 969–976.

Nürnberger, T. and Lipka, V. (2005) Non-host resistance in plants: new insights into an old phenomenon. *Mol. Plant Pathol.* **6**, 335–346.

Peart, J.R., Lu, R., Sadanandom, A. *et al.* (2002) Ubiquitin ligase-associated protein SGT1 is required for host and nonhost disease resistance in plants. *Proc. Natl Acad. Sci. USA*, **99**, 10865–10869.

Podgorski, I. and Sloane, B.F. (2003) Cathepsin B and its role(s) in cancer progression. *Biochem. Soc. Symp.* **70**, 263–276.

Pontier, D., Gan, S., Amasino, R.M., Roby, D. and Lam, E. (1999) Markers for hypersensitive response and senescence show distinct patterns of expression. *Plant Mol. Biol.* **39**, 1243–1255.

Rooney, H.C., Van't Klooster, J.W., van der Hoorn, R.A., Joosten, M.H., Jones, J.D. and de Wit, P.J. (2005) Cladosporium Avr2 inhibits tomato Rcr3 protease required for Cf-2-dependent disease resistance. *Science*, **308**, 1783–1786.

Takahashi, A., Casais, C., Ichimura, K. and Shirasu, K. (2003) HSP90 interacts with RAR1 and SGT1 and is essential for RPS2-mediated disease resistance in Arabidopsis. *Proc. Natl. Acad. Sci.* (USA), **100**, 11777–11782.

Thornberry, N.A. and Lazebnik, Y. (1998) Caspases: enemies within. *Science*, **281**, 1312.

Tian, M., Huitema, E., Da Cunha, L., Torto-Alalibo, T. and Kamoun, S. (2004) A Kazal-like extracellular serine protease inhibitor from *Phytophthora infestans* targets the tomato pathogenesis-related protease P69B. *J. Biol. Chem.* **279**, 26370–26377.

Tian, M., Win, J., Song, J., van der Hoorn, R., van der Knaap, E. and Kamoun, S. (2007) A *Phytophthora infestans* cystatin-like protein targets a novel tomato papain-like cysteine protease. *Plant Physiol.* **143**, 364–377.

Tissier, A.F., Marillonnet, S., Klimyuk, V., Patel, K., Torres, M.A., Murphy, G. and Jones, J.D.G. (1999) Multiple independent defective suppressor-mutator transposon insertions in Arabidopsis: a tool for functional genomics. *Plant Cell*, **11**, 1841–1852.

Tornero, P., Conejero, V. and Vera, P. (1996) Primary structure and expression of a pathogen-induced protease (PR-P69) in tomato plants: Similarity of functional domains to subtilisin-like endoproteases. *Proc, Natl Acad, Sci, USA*, **93**, 6332–6337.

Tornero, P., Conejero, V. and Vera, P. (1997) Identification of a new pathogen-induced member of the subtilisin-like processing protease family from plants. *J. Biol. Chem.* **272**, 14412–14419.

Valentine, T., Shaw, J., Blok, V.C., Philips, M.S., Oparka, K.L. and Lacomme, C. (2004) Efficient virus-induced gene silencing in roots using a modified tobacco rattle virus vector. *Plant Physiol.* **136**, 3999–4009.

Van der Hoorn, R.A.L. and Jones, J.D.G. (2004) The plant proteolytic machinery and its role in defence. *Curr. Opin. Plant Biol.* **7**, 400–407.

Van der Hoorn, R.A.L., Laurent, F., Roth, R. and De Wit, P.J. (2000) Agroinfiltration is a versatile tool that facilitates comparative analyses of Avr9/Cf-9-induced and Avr4/Cf-4-induced necrosis. *Mol. Plant Microbe Interact.* **13**, 439–446.

Van der Hoorn, R.A.L., Leeuwenburgh, M.A., Bogyo, M., Joosten, M.H. and Peck, S.C. (2004) Activity profiling of papain-like cysteine proteases in plants. *Plant Physiol.* **135**, 1170–1178.

Vancompernolle, K., Van Herreweghe, F., Pynaert, G., Van de Craen, M., De Vos, K., Totty, N., Sterling, A., Fiers, W., Vandenabeele, P. and Grooten, J. (1998) Atractyloside-induced release of cathepsin B, a protease with caspase-processing activity. *FEBS Lett.* **438**, 150–158.

Woltering, E.J. (2004) Death proteases come alive. *Trends Plant Sci.* **9**, 469–472.

Xia, Y., Suzuki, H., Borevitz, J., Blount, J., Guo, Z., Patel, K., Dixon, R.A. and Lamb, C. (2004) An extracellular aspartic protease functions in *Arabidopsis* disease resistance signaling. *EMBO J.* **23**, 980–988.

Xu, P., Zhang, Y., Kang, L., Roosinck, M.J. and Mysore, K.S. (2006) Computational estimation and verification of off-target silencing during post-transcriptional gene silencing in plants. *Plant Physiol.* **142**, 429–440.

Zeiss, C.J. (2003) The apoptosis-necrosis continuum: insights from genetically altered mice. *Vet. Pathol.* **40**, 481–495.

